Thermophysics and Aeromechanics, *2020*, *Vol. 27*, *No. 3*

DOI: 10.1134/S0869864320030099

Experimental study of momentum transfer in a cellular flame of rich and lean propane-butane/air mixture*

B.F. Boyarshinov and S.Yu. Fedorov

Kutateladze Institute of Thermophysics SB RAS, *Novosibirsk*, *Russia*

E-mail: boyar@itp.nsc.ru

(*Received October 10*, *2019*; *revised October 30*, *2019*;
accepted for publication November 6, *2019*)

To simulate a cellular flame, rich (equivalent ratio Φ = 1.4) and lean (Φ = 0.9) propane-butane/air mixtures were used in a burner, which forms a stationary flame with a single cell. Experimental data on the temperature fields were obtained using the coherent anti-Stokes Raman scattering (CARS) method; the velocity components were measured using PIV (Particle Image Velocimetry) equipment. The terms of friction stress and static pressure in the momentum transfer equations were calculated using the balance method. It is shown that the equality of dynamic and static pressures associated with the thermal expansion of the combustion products is satisfied on the cellular flame surface. Flameout occurs when the magnitude of the pressure head becomes greater than the magnitude of a static pressure change. The shear stress profiles contain extrema, whose coordinates are associated with streamline curvatures and are close to the position of the heat release region at combustion of lean and rich mixtures.

Key words: cellular flame, non-contact measurements, PIV and CARS methods, momentum transfer.

Introduction

The cellular flame is formed at combustion of gas mixtures and hydrocarbon vapors. As compared to a flat flame front, the surface of cellular flame increases due to the formation of a system of moving hemispherical elements of similar shapes and sizes. This feature allows an assumption that in a cellular flame, the burning rate can increase. Formation of cells during mixture combustion in a tube was noted in [1]; in [2], it was noted above the porous wall; in [3], the cells were observed in the counter-current jets. The authors of [4] associated the formation of such cells with thermal expansion of combustion products. An increase in the volume of combustion products at thermal expansion affects significantly the gas-dynamic characteristics of the flow in the heat release region. According to [5], the streamlines bend at the flame front. At the center of the cell, there is an area of high pressure. In front of the cell, the streamlines diverge, deviating from the rectilinear direction.

In publications on this subject, the theoretical works prevail over the experimental studies. The latter, as a rule, describe the general properties of the object: number of cells, the effect of

* The work was carried out in the framework of the state task to IT SB RAS with partial financial support of the Russian Foundation for Basic Research (Project No. 18-03-00282a).

the flame cellular shape on the burning rate, the dependence of the shape on pressure, geometric and operational parameters. Due to instability of the cellular flame, important characteristics of the zone of chemical transformation become inaccessible. These include static pressure and friction stress distributions. It is shown in [6, 7] that the flame surface is an isotherm; the heat release region corresponds to the maximum of heat flux spent on initial mixture preheating. It is not clear how the combustion zone is connected with momentum transfer and friction stresses. The authors are not aware of experimental studies on the dynamic properties of gas flow near the cellular flame front. Useful information on this issue can be obtained by local measurements of temperature fields, gas composition, and velocity vector components performed with a spatial resolution less than the flame front thickness. The optical methods for measuring temperature and velocity and composition of burning gas with high spatial resolution are known [8]. The methods of processing the results of experiments [9–11] were tested, which made it possible to estimate the terms in the transfer equations based on the balance relations. This work is aimed at obtaining the experimental data on the local velocity and temperature of combustion products in a cellular flame with a spatial resolution of about 0.1– 0.2 mm in application to domestic gas combustion. Further, based on these data, the role of such gas-dynamic parameters as the pressure head and static pressure associated with thermal expansion of gas is analyzed together with friction in a close proximity to the cellular flame front.

1. Object of research

The measurement of local gas parameters near the reacting surface is complicated due to the mobility of cells, which are displaced and deformed when the probes are introduced into the flame. The flame of propane-butane mixture with air rising from a burner, when a dispersed phase is added, is shown in Fig. 1*a*. When measuring the gas velocity by the PIV method, titanium dioxide powder TiO_2 was used. The burner hole with a diameter of 24 mm was covered with a brass mesh. It was shown in [6, 7] that with decreasing hole sizes, the number of cells, as well as their mobility, decreases, and with a diameter of 10 mm (Fig. 1*b*), a single stationary cell suitable for measuring local parameters by optical diagnostic methods was chosen. The flame stabilized over a brass mesh made of a wire of 0.15 mm diameter with a cell size of 0.3×0.3 mm. The same burner was used to study the flame structure of the rich and lean propane-butane/air mixtures (Fig. 1*c*). We used domestic gas; the estimated percentage ratio of propane and butane in it was 75/25 [6]. According to comparison of calibrations, flow rates and

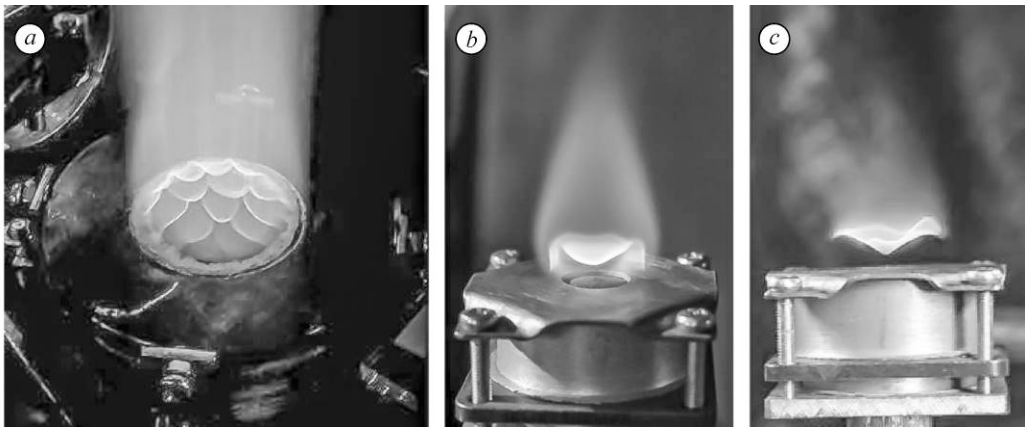

Fig. 1. Multi-cell flame (*a*) and single-cell flame (*b*)
at burning of propane-butane/air mixture (equivalent ratio Φ = 1.4),
flowing upwards from the holes with diameters of 24 and 10 mm, covered by a brass mesh,
lean mixture flame (Φ = 0.9) above the hole of 10 mm diameter (*c*).

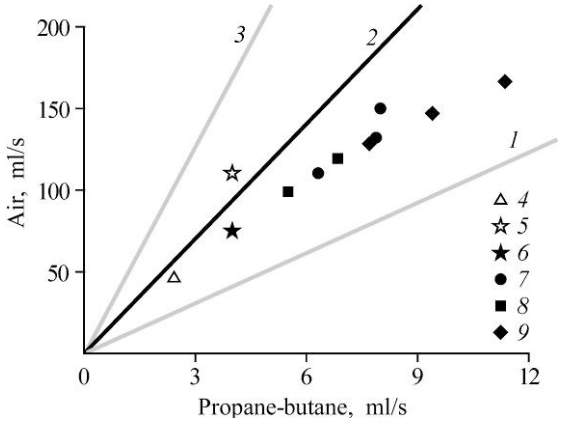

Fig. 2. The ratio of air and propane-butane flow rates corresponding to the generation of cellular flame burning in the jets of various diameters and compositions (according to [6]).
Diameter of the hole:
10 mm (*4*–*6*), 24 mm (*7*), 31 mm (*8*), 40 mm (*9*).

operating parameters of this domestic gas and pure propane (99.9%), they almost coincided. The difference was no more than 5%. The equivalent ratio was estimated in the usual form, as the ratio of volumetric flow rate of combustible gas and air to the corresponding stoichiometric ratio. It was assumed that propane was the main component of fuel.

Data on fuel and oxidizer flow rates in burners with different diameters of initial jets of 10, 24, 31, and 40 mm are presented in Fig. 2. The symbols there correspond to the appearance of cells. Line *2* represents stoichiometric flame, lines *1* and *3* are the known concentration limits of ignition for rich (line *1*) and lean (line *3*) propane-air mixtures. It can be seen that the data for a single flame of rich mixture *6*, obtained for Reynolds number $\mathrm{Re} = d \cdot V / \nu = 370$ and ratio of propane-butane/air flow rates of 4:75(ml/s), are in the same dependence, where the combustion with several cells and equivalent ratio $\Phi = 1.4$–1.6 is presented. This gives the reason to extend the conclusions obtained in the study of the rich mixture flame to other cases of combustion with a multi-cell flame front. The flame of lean mixture *5*, occurring under the conditions of $\Phi = 0.9$, $\mathrm{Re} = 543$, and the ratio of propane-butane/air flow rates (ml/s) of 4:110, was used to assess the effect of combustible mixture composition on momentum transfer.

2. Research objective, method of measurement result processing

The main objective of the study was to obtain experimental data on the flow structure and momentum transfer processes in a vicinity of laminar flames, similar by their characteristics to cellular flames at combustion of upwards jets of rich ($\Phi = 1.4$) and lean ($\Phi = 0.9$) propane-butane mixtures with air. A change in static pressure ΔP and distribution of friction stresses were calculated by the experimental data on the temperature and velocity components. During the research, the gas parameters were compared at combustion of lean and rich mixtures. They were also compared with the position of such characteristic regions in the vicinity of the combustion zone, where the heat release maximum was formed and the glow visualized the flame surface.

To process the obtained experimental data, the balance method, previously used to assess turbulent stresses [9, 10], rate of matter formation [11], and heat release [6] was used. According to this method, the measurement results were presented in the form of a two-dimensional grid of local gas parameters, depending on the jet radius and distance from the burner outlet with a step of 0.125 mm, to obtain two known velocity components and temperature at each node of the grid. The local values of viscosity were determined by temperature. The experimental data prepared in this manner were substituted into the equation of motion, where the derivatives were calculated by the finite differences:

$$\left(\frac{\partial \rho V^2}{\partial y} + \frac{1}{r} \cdot \frac{\partial (\rho r V U)}{\partial r}\right) = -\frac{\partial \Delta P}{\partial y} + \frac{\partial}{\partial y}\left(\mu \frac{\partial V}{\partial y}\right) + \frac{1}{r}\frac{\partial}{\partial r}\left(r \cdot \mu \frac{\partial V}{\partial r}\right) + \Delta \rho g, \qquad (1)$$

here V and U are the components of velocity vector [m/s] in y- and r-direction [m]; ΔP is the change in static pressure [Pa], ρ is the density [kg/m^3], μ is the dynamic viscosity [Pa·s].

Temperature dependences $\mu(T)$ and $\rho(T)$ were taken the same as for nitrogen, whose mass fraction in the mixture for both regions of the gas flow exceeded 77 %. After each differentiation procedure, the calculation results were smoothed by a B-spline, and integration was replaced by summation.

3. Instrumentation

Non-contact methods were used to measure the gas velocity and temperature. A detailed description of applied equipment is given in [6, 7].

3.1. *Measurement of velocity vector projection*

At standard application of PIV equipment, the gas flow is seeded with micron or submicron particles. These chemically inert additives follow the flow without significant slippage. Then the object is illuminated twice by a laser light and two consecutive images are taken. The local flow rate is calculated by changing the position of particles in these images by applying the cross-correlation algorithm.

In accordance with the described algorithm, the particles of TiO_2 powder with approximate sizes from 1 to 5 μm were introduced into the initial gas mixture; these particles passed freely through the metal mesh of the burner to the flame. The particles were illuminated in the laser sheet plane by two Nd:YAG laser radiation pulses with a wavelength of 532 nm and time delay between pulses of 23 μs. The position of particles was recorded by a 4MPix POLIS v1.0 video camera developed on the basis of VIDEOSKAN-4021. The PIV equipment included a POLIS synchronizing processor. Data collection and processing were carried out on a personal computer with ActualFlow software.

The measurements of flow velocity at the outlet hole ($y \sim 1$ mm, $r < 4$ mm) without burning showed that the flow is uniform along the radius with accuracy $\Delta V/V \approx 10$ %. In experiments with combustion, the measuring error for longitudinal velocity component V of TiO_2 particles with a diameter of 1–5 μm, according to the authors' estimates, was (1–9) %. The accuracy of determining the horizontal component U turned out to be lower; therefore, in this work, its value was calculated by the measurements of longitudinal component V through the continuity equation

$$\frac{\partial(r\rho V)}{\partial y} = \frac{-\partial(r\rho U)}{\partial r}. \qquad (2)$$

3.2. *Temperature measurements*

To measure the temperature, we used the method of coherent anti-Stokes Raman scattering (CARS), based on registration of the spectra of radiation excited in the region of intersection of focused laser beams. The equipment used for this method is constructed on the basis of a solid-state Nd:YAG laser with a pulse repetition rate of 10 Hz. Two beams with energies of 12 mJ (with a wavelength of 532 nm), as well as a beam of a tunable dye laser with the energy of 3.5 mJ (with a wavelength of 607.5 nm) were focused and intersected with each other, forming a measuring volume with a characteristic size of 0.1×0.1 mm. The CARS beam arising in the measuring volume was spatially separated from the laser beams; it focused on the outlet slot of a DFS-24 double monochromator with a multichannel optical spectrum recorder. The temperature was calculated by the shape of the spectrum of coherent light scattering on nitrogen molecules using the developed "CARSspectra" program [12].

4. Initial data

The position of the glowing flame surface was determined by photographing, the coordinates of the heat release region were taken from [6]. The symbols in Fig. 3 show the temperature (*1*, *3*) and longitudinal velocity (*2*, *4*) profiles on the cell axis, related to the difference between their initial and final values. Here, $\varphi = (V–V_0)/(V_{max}–V_0)$, $\theta = (T–T_0)/(T_{max}–T_0)$. The distance from the wall "*y*" is related to the hole diameter d = 10 mm. In the flame of rich mixture, V_{max} = 3.12 m/s, V_0 = 0.9 m/s; in the flame of lean mixture, V_{max} = 3 m/s, V_0 = 1.08 m/s. The maximum temperature for both mixtures used is approximately the same and amounts to $T_{max} \sim 2200 \pm 100$ K, which is consistent with the known data [13]. It can be seen that on the axis in front of the cell, the gas decelerates ($\varphi < 0$) as when it flows onto an obstacle, and then accelerates and reaches a maximum at $y/d \sim 1$. The temperature reaches its maximum values at a distance from the wall $y/d \sim$ 0.3–0.35. Obviously, the thermal and chemical changes occur faster than gas-dynamic ones. Apparently, this may be a reason for an increase in static pressure near the cell axis.

5. Results and discussion

To analyze the processes of momentum transfer, the method of balances in the equation of motion (1) was used. A two-dimensional grid of experimental data on velocity, density, and viscosity was used to find derivatives in the momentum equations represented as finite differences. When integrating the equations or their individual parts, the finite differences were summarized.

5.1. *Static pressure*

Using data on the fields of velocity and temperature, we obtained the distribution of static pressure caused by heat generation: $\Delta P = P – P_{atm}$. The profiles of static pressure (*1*) that cause gas expansion are shown in Fig. 4 as a result of integration of the momentum equation (1) along the *y*-axis with the boundary conditions $\Delta P = 0$, if $y = 0$:

$$\Delta P = \int_0^y \left[\frac{\partial}{\partial y}\left(\mu \frac{\partial V}{\partial y} \right) + \frac{1}{r} \cdot \frac{\partial}{\partial r}\left(r \cdot \mu \frac{\partial V}{\partial r} \right) - \left(\frac{\partial \rho V^2}{\partial y} + \frac{1}{r} \cdot \frac{\partial (\rho r V \cdot U}{\partial r} \right) + \Delta \rho g \right] dy. \qquad (3)$$

It is obvious that in the case of rich mixture (Fig. 1*b*), a limited region, where the static pressure ΔP_{st} exceeds the ambient pressure and becomes lower than the atmospheric one at the cell outlet (y > 5 mm), is formed near the cell axis. The noted features relate also to lean mixture burning (Fig. 1*c*). The position of curve intersection is on the visible flame surface (dark square). Symbols *2* in Fig. 4 show the profiles of a change in the pressure head $\Delta P_{dyn} = \rho V^2/2$ near the cell center for r = 0.5 mm. In a cellular flame, the pressure heads are low (of about 0.1–1 N/m^2) and comparable with changes in the static pressure, which explains the known difficulties with the use of pneumatic probe methods to study hydrodynamics of such objects.

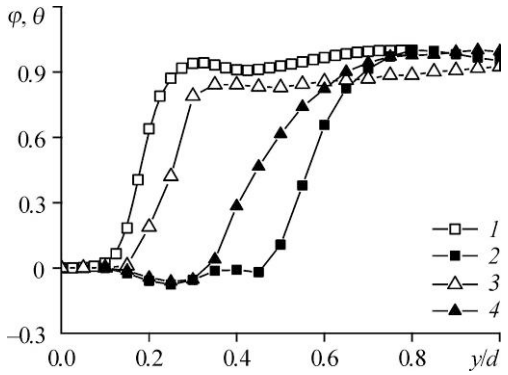

Fig. 3. Profiles of longitudinal velocity and temperature of rich and lean flames on the cell axis. Mixtures: rich (*1*, *2*) and lean (*3*, *4*); profiles temperature of θ (*1*, *3*) and longitudinal velocity φ (*2*, *4*).

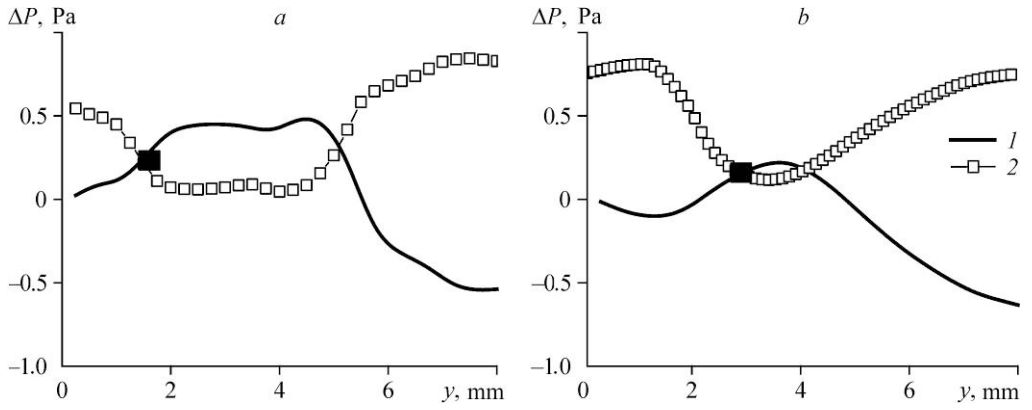

Fig. 4. Distribution of static pressure at combustion of rich (*a*) and poor (*b*) propane-butane mixtures with air for $r = 0.5$ mm.
Static pressure (*1*), dynamic pressure (*2*), position of the visible flame surface is the dark square.

The convergence of the pressure head level and increased static pressure is a condition for holding the flame, i.e., $\Delta P_{dyn}/\Delta P_{st} \sim 1$. With a further increase in the flow rate of mixture (Fig. 4*b*), the pressure head can overcome the static pressure, and flameout will occur. With a decrease in the pressure head, the flame front propagates towards the oncoming mixture flow.

5.2. *Flow pattern in a flame cell of propane-butane/air mixture*

By definition, the stream function ψ is found by integrating expression $\rho V = (1/r)\times$ $\times(\partial\psi/\partial r)$, then the flow pattern is constructed from the condition $\psi = \int_0^r \rho V r\, dr = \text{const}$. Here, integration was also replaced by the summation of finite differences. Based on the experimental data, we obtained a general picture of distribution of gas-dynamic and thermal parameters. Isobars, streamlines, and visible flame profile of a rich propane-butane mixture with air are shown in Fig. 5 taken from [6]. The streamlines show the jet boundaries, "impermeable" to the convective gas motion. It is seen that in front of the cell, the flow becomes diverging, and at a distance from the grid, the streamlines are turned towards the cell axis. The general nature of the flow is similar to the flow around an obstacle with free boundaries, which is the region of increased static pressure that occurs during thermal expansion of combustion products.

5.3. *Friction near the flame front*

Let us consider the effect of the initial mixture composition on friction near the flame front. It is shown in [6] that there is no rotational motion in the cellular flame; therefore, two projections of shear stresses are equal to zero: $\tau_{y\varphi} = \tau_{r\varphi} = 0$. According to [14], the component of the stress tensor τ_{yr} is determined by the formula

$$\tau_{yr} = \mu\left(\frac{\partial U}{\partial y} + \frac{\partial V}{\partial r}\right). \tag{4}$$

Profiles $\tau_{yr}(y)$ in the flames of rich (*1*) and lean (*2*) mixtures are presented in Fig. 6 for $r = 2$ mm. Line *3* shows the stress level in the laminar boundary layer [14] for the case of air flowing around the wall with $V_0 = 1$ m/s without burning: $\tau = 0.332(yV_0/\nu_0)^{-0.5}\rho_0 V_0^2$. It is seen that the absolute values of shear stresses in the flame can exceed their level in the standard

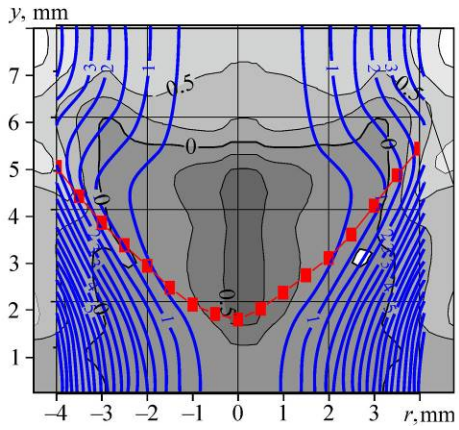

Fig. 5. Pattern of the flow around a cell at rich mixture burning.
Streamlines (blue lines), flame profile (red squares), isobars (black lines) in the flame of rich propane-butane mixture with air.

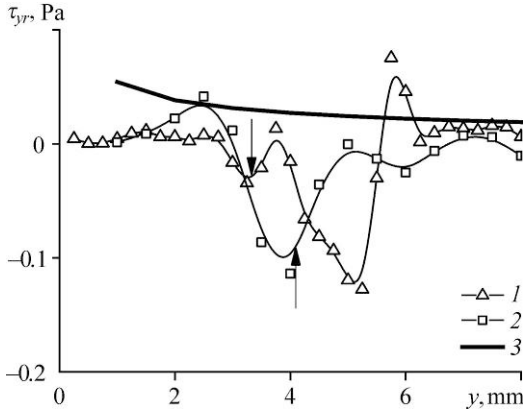

Fig. 6. Shear stresses at burning of rich and lean propane-butane mixtures with air.
Burning of rich (*1*) and lean (*2*) mixtures; shear stress in the laminar boundary layer without burning (*3*).

laminar boundary layer. In each profile, there are the extremes reflecting the effect of thermal expansion. The arrows indicate the position of the heat release region, which in the cases of combustion of rich and lean mixtures coincides with the minima in the stress profiles. Other extrema are associated with a change in the curvature of streamlines (for combustion of a rich mixture, the flow pattern is shown in Fig. 5).

Conclusion

The purpose of the work was to study a three-dimensional non-stationary cellular flame and obtain data on dynamic parameters and their dependences on the initial mixture composition. It is known that the flame front is characterized by a small thickness of the region of chemical transformations (~ 1.5–2.0 mm), high temperature gradients, and problems associated with the use of conventional methods of probe diagnostics. The source object, i.e., non-stationary cellular flame, was replaced by its analogue: a burner, which creates flame in the form of a separate stationary cell available for non-contact measurements. This flame was studied using the CARS and PIV optical equipment; as a result, the data on the velocity and temperature fields during combustion of rich (equivalent ratio $\Phi = 1.4$) and lean ($\Phi = 0.9$) propane-butane/air mixtures were obtained. Distributions of parameters for these flames were compared with each other and with the position of such characteristic regions in a vicinity of the combustion zone, where the maximum heat release was established and where the glow visualized the flame surface. To obtain information on gas-dynamic parameters that are not available in direct measurements, the obtained experimental data were processed using the method of balances in the equation of motion.

It was established that the rate of temperature increase from the initial to the final value exceeds significantly the rate of the gas velocity increase, which may be a reason for a local increase in static pressure associated with thermal expansion directly behind the flame front. On the glowing flame surface, the increased static pressure equals the pressure head. When the pressure head exceeds the static pressure due to thermal expansion of gas, a flameout occurs. The coordinates of extrema in the shear stress profile are close to the position of the heat release region during combustion of the lean and rich mixtures. Extrema also demonstrate a connection with the curvature of streamlines; their scale can exceed the level of stresses in the flows without combustion.

An approach that takes into account the relationship between dynamic and static pressures can be applied for the analysis of the phenomena of flame propagation and stability and safety of the combustion process ("breakthrough", flameout, etc.). The accuracy of conclusions depends not only on the measurement location and equipment features, but also on the method of result processing. We should note that the balance method was tested in [9] by experimental data of [15] on turbulent stresses without combustion. Satisfactory agreement with the data of [16] on turbulent heat fluxes around a flat plate was achieved. In experiments with a cellular flame, the error of the balance method can be established only in individual cases. For instance, on the visible flame surface, the error in the static pressure is comparable to the error in the pressure head, i.e., it does not exceed 10–15%. The research results can be supplemented and refined as experimental equipment and methods for processing measurement results are improved.

References

1. **B. Lewis and G. Elbe,** Combustion, Flames and Explosions of Gases, Academic Press, New York, 1961.
2. **J.P. Botha and D.B. Spalding,** The laminar flame speed of propane/air mixtures with heat extraction from the flame, in: Proc. R. Soc. London, Ser. A, 1954, Vol. 225, No. 1160, P. 71–96.
3. **E. Korusoy and J.H. Whitelaw,** Extinction and relight in opposed flames, Exp. Fluids, 2002, Vol. 33, P. 75–89.
4. **L. Landau,** On the theory of slow combustion, J. Exp. Theor. Phys., 1944, Vol. 14, iss. 6, P. 240–245.
5. **A.N. Lipatnikov and J. Chomiak,** Effects of premixed flames on turbulence and turbulent scalar transport, Prog. Energy and Combust. Sci., 2010, Vol. 36, P. 1–102.
6. **R.Kh. Abdrakhmanov, B.F. Boyarshinov, and S.Yu. Fedorov,** Investigation of the local parameters of a cellular propane/butane/air flame, Inter. J. Heat and Mass Transfer, 2017, Vol. 109, P. 1172–1180.
7. **B.F. Boyarshinov, S.Yu. Fedorov, and R.Kh. Abdrakhmanov,** Experimental investigation of structure and heat transfer in cellular flame of propane/butane/air mixtures, Thermophysics and Aeromechanics, 2019, Vol. 26, No. 1, P. 79–88.
8. **C.K. Law and C.J. Sung,** Structure, aerodynamics, and geometry of premixed flamelets, Progr. Energy and Combust. Sci., 2000, Vol. 26, P. 459–505.
9. **B.F. Boyarshinov, V.I. Titkov, and S.Yu. Fedorov,** Momentum transfer in the boundary layer when there is acceleration and combustion of ethanol as it evaporates behind a barrier, Combustion and Flame, 2010, Vol. 157, P. 1496–1509.
10. **B.F. Boyarshinov,** Investigation of momentum transfer in the turbulent boundary layer with ethanol combustion behind a barrier: the effect of external flow turbulence, in: Abstracts XVI ICMAR Conf. Part I, Russia, Kazan, 19–25 August, 2012, P. 62–63.
11. **B.F. Boyarshinov,** Investigation of momentum and mass transfer in the turbulent boundary layer with ethanol combustion behind a barrier, Nonequilibrium Processes in Plasma, Combustion, and Atmosphere, A.M. Starik, S.M. Frolov (Eds.), Torus Press Ltd., Moscow, 2012, Vol. 482, P. 221–227.
12. **S.Yu. Fedorov,** CARSspectra v.02: Certificate No. 2017616085 Russian Federation; registered in the Computer Software Registry on June 1, 2017, http://www.itp.nsc.ru/Laboratory/LAB_2_1/Methods/index.html.
13. **V.M. Maltsev, M.I. Maltsev, and L.Ya. Kashporov,** Main Characteristics of Combustion, Khimiya, Moscow, 1977.
14. **H. Shlichting,** Boundary Layer Theory, McGraw-Hill, New York, 1968.
15. **H.H. Fernholz, E. Krause, M. Nockemann, and M. Schober,** Comparative measurements in the canonical boundary layer at $Re_{\delta 2} \leq 6\times10^4$ on the wall of the German-Dutch windtunnel, Phys. Fluids, 1995, Vol. 7, No. 6, P. 1275–1281.
16. **H.W. Coleman, R.J. Moffat, and W.M. Kayes,** Momentum and Energy Transport in the Accelerated Fully Rough Turbulent Boundary Layer, Report No. HMT-24, Stanford University, 1976.